PERGAMON

Available online at www.sciencedirect.com

SCIENCE DIRECT®

Acta Astronautica 57 (2005) 341–347

ACTA ASTRONAUTICA

www.elsevier.com/locate/actaastro

Development of a differential accelerometer to test the equivalence principle in the microscope mission

D. Hudson*, R. Chhun, P. Touboul

Department of Physics & Instrumentation, Office National d'Etudes et de Recherches Aérospatiales, Châtillon, France

Available online 18 April 2005

Abstract

A violation of the Equivalence Principle (EP), which hypothesizes the equality of inertial mass and gravitational mass, is indicated by current theories in modern physics. The MICROSCOPE mission seeks to extend the accuracy of previous EP tests to 10^{-15}, by avoiding the disturbances inherent to every Earth based test facility. The test will involve the measurement of the electrostatic forces required to maintain two concentric masses on the same orbit. The satellite, to be launched in 2008, will carry two differential accelerometers, one with masses of platinum and titanium, and a second with two platinum masses for baseline measurements. Each accelerometer will contain two coaxial cylindrical proof masses, each encompassed by a silica cage, all in a vacuum housing. The capacitance between electrodes etched into the silica, and the surface of the gold-coated proof masses provides a measurement of the proof mass position, which is then controlled by adjusting the voltages applied to the electrodes. Because an EP violation will appear as a difference between the forces required to keep each mass centred, the quality and stability of the silica cages is essential to achieve the desired test accuracy. This paper presents the overall design of the accelerometer, focusing on areas critical to the instrument core design, integration, and final performance requirements. The models and experimental investigations designed to overcome these issues are also discussed.
© 2005 Elsevier Ltd. All rights reserved.

1. Introduction

In 1911, Einstein proposed his Principle of Equivalence, postulating the equality of gravitational mass and inertial mass. In the years since, this theory has been tested using numerous methods, but the noise and vibrations inherent in any Earth-bound test environment have restricted the test accuracy to less than 10^{-13}. Recent efforts to obtain a unification theory of fundamental forces have renewed interest in disproving the Equivalence Principle (EP), and present day satellite technology provides an opportunity to perform EP tests with unprecedented accuracy.

The MICROSCOPE mission (a French acronym for MICROSatellite à traînée Compensée pour l'Observation du Principe d'Equivalence) intends to verify the EP to 10^{-15} by placing two test masses of different materials on the same orbit to within

* Corresponding author. Tel.: +33 1 46 73 47 88; fax: +33 1 46 73 48 24.

E-mail addresses: hudson@onera.fr (D. Hudson), chhun@onera.fr (R. Chhun), touboul@onera.fr (P. Touboul).

0094-5765/$ - see front matter © 2005 Elsevier Ltd. All rights reserved.
doi:10.1016/j.actaastro.2005.03.017

10^{-11} m. They will be maintained on the same orbit by means of electrostatic forces and a difference in the required forces will indicate an EP violation.

The mission is approved and funded under the CNES MYRIADE microsatellite programme, which places restrictions on the payload size and power consumption. This constrains the experiment design, allowing only two science instruments and prohibiting the use of cryogenics. One will contain proof masses of two different materials for the EP test, while the other will have two masses of the same material to provide a science baseline.

Performing this test in space greatly reduces the experiment noise. In addition to having none of the seismic vibrations of an earth bound lab, remaining vibration sources are further reduced by a drag compensating satellite control system. The space environment also allows a long measurement duration. By integrating over many orbits the signal to noise ratio can be significantly improved. Performing this test in space offers another advantage besides low noise levels: the frequency at which an EP violation may appear is well known, being the sum of the orbit frequency and the frequency of any spin of the measurement axis in the orbit plane. The experiment will therefore be performed in both inertial mode, with the satellite attitude fixed in inertial space, and spin mode, with a controlled, constant rate of spin applied to the satellite, in order to increase the frequency of the EP violation signal.

The two SAGE (Space Accelerometer for Gravitation Experimentation) accelerometers for MICROSCOPE are based on a successful heritage of high sensitivity electrostatic accelerometers developed by ONERA, including STAR, used on the CHAMP mission [1], and SuperSTAR, for the GRACE mission [2]. The differential accelerometer, however, is a step away from previous instruments due to the necessity of positioning two proof masses with a common centre of mass. This paper provides a detailed description of the SAGE instrument followed by a discussion of various design details critical to reach the targeted 10^{-15} accuracy. Finally, Section 4 provides an overview of the various models and tests used in the development process.

2. The differential electrostatic accelerometer

An electrostatic accelerometer consists, fundamentally, of a proof mass suspended in a highly stable electrode cage. The principle of operation is to measure the electrostatic forces required to maintain the position of the proof mass with respect to the electrodes. Because the suspended proof mass is, in the nominal operation of a perfect instrument, susceptible only to the field forces of gravity and the electrostatic forces applied by the electrodes, the latter is proportional to the difference between the total acceleration of the cage and the gravitational acceleration of the proof mass. In the differential model, the two electrode cages experience the same acceleration, so that in the differential measurement the cage accelerations cancel to leave only the difference between the gravitational acceleration of the two masses.

There are three components to each SAGE instrument. The sensor unit (SU) contains the two inertial sensors carefully aligned in a vacuum tight housing. This is electrically connected to the front end electronics unit (FEEU), which contains the low noise analogue electronics required for proof mass levitation, including the ADCs, DACs, and position sensors, which require more thermal stability than the digital electronics of the interface control unit (ICU). This latter unit contains the remaining electronics for SU operation, specifically the proof mass position control loop, as well as the systems for general experiment control and the satellite interface.

2.1. Sensor unit

The objective of the MICROSCOPE mission is to compare the effect of gravity on two masses of different material, which requires subjecting them to the same gravitational field simultaneously. To achieve this in the variable field of Earth's gravity two restrictions are placed on the accelerometer design: the masses must be concentric to share a common centre of gravity, and the shape of the masses must be chosen so that the gravity gradient effects are analogous on the two masses. Optimally, the masses would be gravity monopoles [3], such as spherical shells, but as a more practical choice the SAGE instrument uses concentric cylinders. This enables access to the inner mass, and dimensions which produce equal

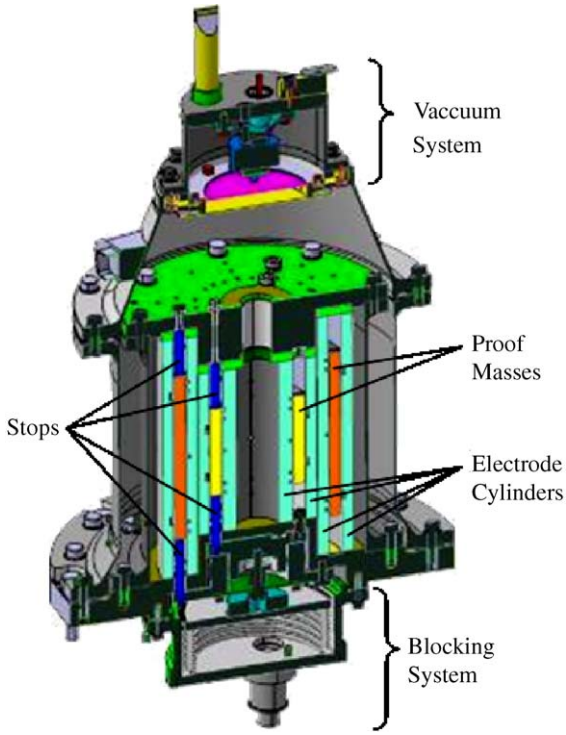

Fig. 1. MICROSCOPE sensor unit cross section.

second order moments of inertia on each axis guarantee a sufficient rejection of self gravity perturbations of the satellite.

The sensor core of SAGE is therefore composed of two concentric, coaxial, cylindrical proof masses. The instrument providing the science base line has both masses in platinum–rhodium, while the EP test instrument has the external mass in titanium and the internal in platinum–rhodium. The titanium mass has a nominal length of 79.9 mm, outer radius of 35 mm, and a mass of 364 g, while the smaller platinum mass has nominal dimensions of 43.5 mm in length and 20 mm in outer radius, and a mass of 473 g. Each mass has a set of electrodes sufficient to control all six axes of motion (three linear, three rotational) engraved onto gold plated silica cylinders within and without the proof mass, which are shown in Fig. 1.

To enable the capacitive position measurement and control, a sinusoidal voltage is applied to the proof mass via a fine gold wire, which is required to control the charge on the proof mass and is the only physical

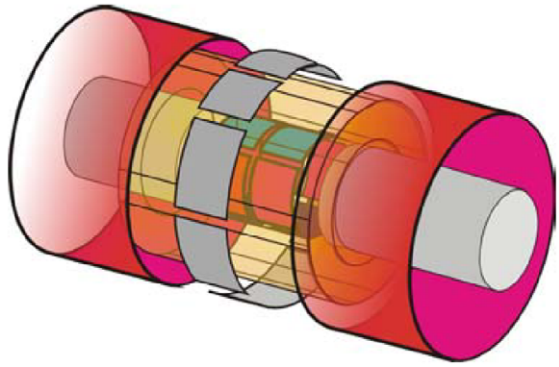

Fig. 2. Layout of electrodes about the proof mass.

connection between the proof mass and its electrode cage. Three stops at each end of the PM cylinder limit the motion along and about the cylinder axis to prevent stress on the gold wire. At one end the stops are mobile, to support the proof mass during launch but allow motion once in orbit. Stops placed on the interior electrode cylinder prevent contact between the proof mass and electrodes, however these stops are only necessary before control is obtained, or in the case of a loss of position control. The core of proof masses and electrode cylinders are mounted on a base plate which is designed to ensure precise alignment of the six cylinders during assembly. This assembly is enclosed by a double walled housing in which a vacuum is maintained.

2.2. Electrodes

The same electrodes are used simultaneously for both position sensing and position control, and are positioned as shown in Fig. 2. The inner cylinder contains four independent pairs of electrodes for the two radial axes and the rotations about these axes, so that each measurement is an average of two pairs and the same two pairs act in conjunction for position control. The outer cylinder contains eight pairs of electrodes around the centre which act in unison for measurement and control of the rotation about the cylinder axis. This is possible thanks to four narrow flattened areas on the outside of the proof masses. The electrodes for the sensitive axis are also on the outer cylinder, covering the entire circumference at either end.

The cylindrical accelerometer is much more complex than previous parallelepiped versions [4]. The curvature results in a variation in separation across the electrode if the PM is not perfectly centred. Therefore the expressions for force and capacitance must be integrated over the area of the electrode. Besides the equations becoming more complex, control is more difficult as the electrode curvature causes coupling between the axes [5].

2.3. Position control loop

To each pair of electrodes is connected a position detector which converts the difference in capacitance from the two electrodes to a voltage via a differential transformer. This voltage is digitized and input to the control laws which can be based on a standard PID loop. The output from the control is applied to both electrodes, but with opposite signs. Because the proof mass is held at a steady voltage via the gold wire, the electrodes apply an electrostatic force to the mass which is proportional to the electrode voltage when the configuration is symmetric. The symmetric application of the electrode voltages also avoids coupling between linear and rotational motion, thus allowing position control on all six axes. The science data from the sensitive axis is sampled after the final amplifier in the loop to reject the noise from all the loop components, including this drive voltage amplifier and the DAC.

3. Mission critical design considerations

3.1. Alignment to gravity field

The altitude of the satellite is provided by a star camera with which the sensor units are precisely aligned via an optical cube on their base plate. The stability of this alignment is, however, dependent on the rigidity and thermal sensitivity of the satellite bus. The sensor units themselves are carefully assembled and mounted on the base plate to provide precise alignment of the core cylinders with the optical cube, and the material of the sensor unit is chosen for its thermal stability.

To reject Earth's gravity gradient effects from the differential measurement, the gravity gradients must be computed in the instrument reference frame. Great care is taken to ensure the stability of the alignment described above because the star camera outputs are used to estimate the orientation of the measurement axis.

Table 1
Errors in scale and bias for each inertial sensor, due to thermal variations in the SU or FEEU and expressed in $\mathrm{m\,s^{-2}/K}$. Inertial sensor 1 is interior to inertial sensor 2 in the differential accelerometer

	SU	FEEU
Sensor 1 bias error	1.76×10^{-13}	6.25×10^{-14}
Sensor 1 scale error	2.26×10^{-13}	7.05×10^{-14}
Sensor 2 bias error	1.83×10^{-13}	4.73×10^{-14}
Sensor 2 scale error	1.92×10^{-13}	7.05×10^{-14}
Total error	7.77×10^{-13}	25.08×10^{-14}

3.2. Thermal stability

In addition to the star camera alignment, temperature variations of the instrument affect both the electronic systems and the physical properties of the sensor core. To maintain the performance requirement of better than $8 \times 10^{-15}\,\mathrm{m/s^2}$, the temperature variation of each component is limited. At the EP test frequency, these are $\pm 3\,\mathrm{K}$ for the ICU, $\pm 10\,\mathrm{mK}$ for the FEEU, and $\pm 1\,\mathrm{mK}$ for the SU.

The thermal control of the microsatellite is performed entirely by passive methods, which is possible thanks to the heliosynchronous orbit which minimizes the thermal variations. The more sensitive SU and FEEU are insulated from the other satellite components to reduce temperature variability and the vacuum and double walled housing of the SU further insulates the core mechanics.

Thermal variations result in an error in the bias and scale factors of the instrument output. Each axis of each inertial sensor has its own bias and scale which depend on various properties and components such as the cylindricity of the proof mass, the capacitive position sensor, the electrode symmetricalness, the gold wire damping, and the drive voltage amplifier gain and bias. The effect of temperature variations on each contributor has been analysed for temperature variations of the SU and FEEU, with the results summarized in Table 1. To enable comparison, the bias errors were

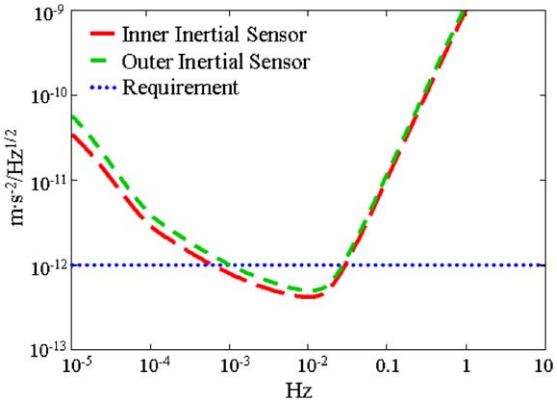

Fig. 3. Instrument resolution along the sensitive axis.

converted to units of acceleration from acceleration per volt using the voltage corresponding to an estimate of the expected acceleration on orbit, $2.5 \times 10^{-7}\,\mathrm{m/s^2}$.

3.3. Instrument resolution

The frequency range of interest is defined by the frequency of a possible EP violation. At minimum this is 1.7×10^{-4} Hz corresponding to the orbit frequency of the satellite, and will be increased by operating in spin mode as described in Section 1. The resolution of the inertial sensors along the sensitive axis is described by Fig. 3, which has been created by examining the resolution of each component. The higher frequency operation, above 2×10^{-2} Hz, is limited by the resolution of the capacitive sensor, while lower frequency operation, below about 3×10^{-3} Hz, depends on the gold wire damping. The lowest resolution is between these regions, where the performance is limited by the drive voltage amplifier. The thermal sensitivity of the bias becomes the limiting factor below 10^{-4} Hz, but this is below the frequency range of interest.

The target resolution required to achieve the 10^{-15} test accuracy is $10^{-12}\,\mathrm{m\,s^{-2}/Hz^{1/2}}$, when considering a signal integrated over more than eight orbits. At the first planned spin frequency of 7.9×10^{-4} Hz, this resolution is attained. However, at the lower frequency of the inertial mode a longer integration time is required to attain the desired EP test accuracy. Fig. 3 shows that the outer sensor is just over target, at $1.1 \times 10^{-12}\,\mathrm{m\,s^{-2}/Hz^{1/2}}$, but the inner sensor is sufficiently under target to compensate. With an integration time of 1.2×10^5 s the differential signal at this frequency will have a maximum resolution of 6×10^{-16}.

3.4. Launch stress durability

To avoid damage to the sensor unit during launch, each proof mass is supported by three stops at each end of the cylinder. At one end, a blocking system applies 2400 N to the three stops during launch to prevent slippage between the stops and proof mass, and once in orbit it retracts the stops a few microns to allow SU operation. The stops are designed to provide sufficient support to prevent contact between the proof masses and electrode cylinders. Besides the effectiveness of the support, the greatest design concern for the blocking system is that the proof mass can be released without the stops sticking to or otherwise damaging it.

A preliminary analysis has been performed via numerical modelling to determine how much movement the stops permit. With an expected maximum acceleration during launch of 20 g applied to both the proof mass and all six stops in a uniform direction normal to the cylinder axis, the maximum displacement was found to be 23.4 μm for the external mass of platinum, which is the most massive, with any orientation of the three stops. As the smaller separation between the proof mass and internal cylinder stops is 145 μm, this is considered a safe amount of motion. A complete verification of the blocking system design will be obtained through vibration testing of the flight qualification test model (described in Section 4.3).

4. Development process

The highly sensitive accelerometer requires the microgravity environment of Earth orbit for suspension of the proof masses. As a result, the instrument designed for in-flight operation cannot be fully tested prior to flight. Instead, a series of models adapted for ground based testing are developed to verify the performance and calibration. These begin with a non operational version for mechanical and electrical testing, followed by simplified designs for artificial levitation on ground, and models for operation only in the Bremen drop tower.

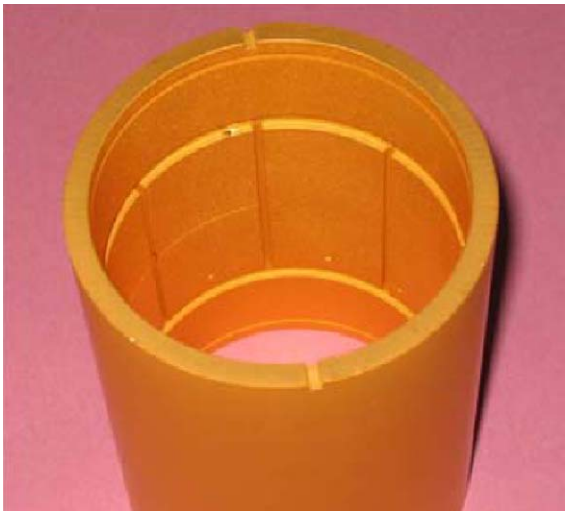

Fig. 4. External electrode cylinder of the mechanical test model external inertial sensor.

4.1. Mechanical test model

The purpose of this model is to verify the construction capabilities, with respect to machining the parts with sufficient accuracy, as well as the ability to assemble the sensor unit with sufficient precision. No performance tests will be performed as this model does not have a functioning inertial sensor. The final accelerometer design must balance performance requirements with machining capabilities, but the design has not yet been limited by production capabilities. Fig. 4 shows one of the gold plated silica electrode cylinders which has been produced for the mechanical test model.

4.2. Prototype model

The primary objective of the prototype is to provide evidence that a cylindrical test mass can be controlled by this electrode configuration, and determine if any additional restrictions are required on the control loops. Therefore it contains only a single inertial sensor, with an analogue control loop based on the circuit used for other accelerometers developed at ONERA. It is adapted for operation in 1 g and the objective will be considered attained when the proof mass is successfully levitated by the electrostatic forces. Further testing on this model may be performed as a means of preparing for future analysis of the differential models.

To enable levitation on ground, the prototype proof mass is made of gold plated silica, weighing only 14 g. The electrode layout is the same as the flight model with the exception of the rotation electrodes on the outer cylinder. Only two flat areas are used for rotation control, and two larger electrodes replace the four electrodes which are not used. These larger electrodes provide a supplemental force to assist with levitation. In addition, the dimensions of the instrument are different from those of the flight model to produce smaller gaps of only 40 or 50 μm between the proof mass and electrodes, as smaller separation allows a greater levitation force from the same applied voltage.

4.3. Subsequent models

The engineering model will be a full differential model with the same dimensions as the flight model. However, the proof masses will both be in silica to allow artificial levitation. This design will test the digital control loop and differential measurement operations, as well as the performance requirements and calibration techniques.

The qualification model will be used for full vibration and thermal testing. This requires high density proof masses comparable to those used for the flight model. It will also be a full differential model completely conforming to the flight model design, and will only be operational as an inertial sensor during free fall testing in the Bremen drop tower. The free fall tests will essentially be full EP tests of a few seconds duration.

The two flight models, one with platinum–rhodium and titanium masses, the other with two platinum–rhodium masses, will be subjected to more limited vibration testing and calibration tests to the extent possible on ground. Operation of these will not be possible on ground, but they will be dropped in the free fall tower prior to launch.

5. Conclusion

To test the Equivalence Principle (EP) to a precision of 10^{-15}, a differential electrostatic accelerometer is in the process of development. This

accelerometer maintains two concentric coaxial cylindric proof masses on a common orbit with electrostatic forces, and any difference in the required force indicates a difference in the effect of gravity. Performing this test in space offers many advantages, including knowledge of the frequency at which a violation will appear. This frequency can be chosen by spinning the satellite in its orbit plane.

A number of issues essential to mission success have been discussed. To reach the 10^{-15} target requires precision and stability of both mechanical and electrical systems. The precision of the mechanical system is achieved through exact machining and careful alignment during assembly, while the stability of mechanical alignments and electronic responses is achieved through the use of components with a low temperature sensitivity and low thermal variations on the satellite. The resulting error due to temperature change is well within the target limits. The instrument resolution is also essential to achieve the 10^{-15} accuracy, but the ability to extend the integration time permits a relaxation of the resolution requirements, or, on the other hand, the possibility of achieving a better test accuracy. To ensure the instrument endures the launch vibration without damage, a blocking system has been designed to support the proof masses until orbit is attained, when it will release the masses.

Because the flight models are designed to operate in a microgravity environment their performance cannot be directly verified before launch. Instead, a series of adapted models are used to indirectly verify the performance through specific experimental procedures with specialized facilities such as the Bremen Drop Tower. However the in-flight calibration is essential to ensure that the linear combinations of the differential measurements are performed with accurate sensitivity factors to fully reject any common applied accelerations larger than 10^{-15} g. The two final models, one for a science baseline and the other for the EP test, will be launched on a CNES microsatellite in early 2008.

Acknowledgements

The authors would like to acknowledge the support of the CNES MICROSCOPE team, especially Sylvie Leon and Jean-Bernard Dubois. Additionally, the primary author would like to acknowledge financial support from both ONERA and CNES.

References

[1] C. Reigber, H. Luehr, P. Schwintzer, CHAMP mission status, Advanced Space Research 30 (2) (2002) 129–134.
[2] E. Davis, et al., The GRACE mission: meeting the technical challenges, in: 50th International Astronautical Congress, IAF-99-B.2.05 Conference, 1999, AAS 90-034.
[3] E. Willemenot, Pendule de torsion à suspension électrostatique, très hautes résolutions des accéléromètres spatiaux pour la physique fondamentale, Ph.D. Thesis, Université de Paris-Sud U.F.R. Scientifique d'Orsay, 1997.
[4] P. Touboul, et al., Accelerometers for CHAMP, GRACE, and GOCE, Bol. Di Geof. Teor, Ed Appl. 090, 2000.
[5] L. Lafargue, Configuration méchanique d'accéléromètres électrostatiques pour le test en orbit du principe d'equivalence, Ph.D. Thesis, Université Paris VI Pierre et Marie Curie, 2002.